Journal of Catalysis **196,** 212–223 (2000)
doi:10.1006/jcat.2000.3034, available online at http://www.idealibrary.com on IDEAL®

Active Sites in Fe/MFI Catalysts for NO_x Reduction and Oscillating N_2O Decomposition

El-M. El-Malki, R. A. van Santen,[1] and W. M. H. Sachtler[2]

V.N. Ipatief Laboratory, Center for Catalysis and Surface Science, Department of Chemistry, Northwestern University, Evanston, Illinois 60208

Received December 27, 1999; revised August 10, 2000; accepted August 15, 2000

Fe/MFI catalysts prepared either by sublimation of $FeCl_3$ onto H-MFI or by solid state ion exchange were characterized by XRD, FTIR, and ESR spectroscopy. Ligated Fe^{3+} ions, such as $(Fe(OH)_2)^+$ or $(Fe{=}O)^+$ in distorted tetrahedral coordination, multinuclear oxocations, such as $(HO{-}Fe{-}O{-}Fe{-}OH)^{2+}$, and Fe_2O_3 oxide particles have been identified. Their relative abundances depend on the Si/Al ratio and the Fe loading. Nitro and nitrate groups, identified by their FTIR bands, are formed upon exposing Fe/MFI with high Fe loading to N_2O. These adsorption complexes are reduced with benzene at 200°C but not at room temperature. Their reduction with CO occurs at a lower temperature than that of the bridging oxygen. Exposure to N_2O at 320°C and 0.5 kPa pumps 30% more active oxygen into Fe/MFI than calcination in O_2 of 100 kPa at 500°C. Thermal decomposition releases NO and O_2 at the same temperature. The catalytic decomposition rate of N_2O to $N_2 + \frac{1}{2}O_2$ in diluted feed streams over Fe/MFI is first order in N_2O. The rate constant is very low for samples with low Fe loading, but jumps to a much higher value for high Fe loadings, indicating the important role of multinuclear Fe clusters in accordance with recent EXAFS results. Stable isothermal oscillations are observed with overexchanged Fe/MFI (Fe/Al = 1; Al/Si = 1/14), in the presence of H_2O vapor, showing that two different states of catalytic activity exist. No oscillation is observed with a dry feed or over Fe/MFI with low loading.

Key Words: **Fe/MFI catalysts; nitrous oxide decomposition; catalytic oscillations; binuclear Fe oxoions; nanoclusters.**

INTRODUCTION

Incorporation of transition metal ions into zeolite cavities leads to materials with interesting properties, in particular, for heterogeneous catalysis. Fe-exchanged zeolites have been reported to display high activity for the selective oxidation of benzene to phenol with N_2O as the oxidant (1, 2). Other representatives of this class are known to be active in the selective catalytic reduction (SCR) of nitrogen oxides, such as those present in the emission from lean burn engines (3–5). Fe/MFI is also known to catalyze the decomposition of N_2O (6, 7). There is little definitive evidence in the literature on the precise nature of the sites responsible for this catalysis. It is even unclear whether or not the same sites are used in N_2O decomposition, benzene oxidation, and the SCR of NO_x.

Cations in zeolite cavities compensate the negative charge of Al-centered tetrahedra in the lattice. For threefold positive ions such as Fe^{3+}, full charge compensation can be achieved at a maximum loading of $Fe^{3+}/Al = 1/3$. However, higher metal loading is possible if part of the positive charge is compensated by extralattice anions, such as extralattice oxygen. Experimentally, high metal loadings such as $Fe^{3+}/Al = 1$ are achieved by subliming $FeCl_3$ vapor onto the acid form of the zeolite. In this case, the primary deposition step is a chemical reaction of $FeCl_3$ with the zeolite protons, leading to the formation of HCl and primary deposits such as $[FeCl_2]^+$ ions. FTIR data show that these positively charged groups replace all original Brønsted sites, indicating a highly homogeneous distribution over all exchange sites in the zeolite. In subsequent hydrolytic steps the Cl^- ligands can be replaced by OH^- groups, so that after calcination the Fe^{3+} ions are surrounded by oxide and/or hydroxide groups in addition to zeolite oxygens. In this situation, each ligated Fe^{3+} ion compensates the charge of one Al-centered tetrahedron. Such overexchanged Fe/MFI materials are very active catalysts for the SCR of NO_x. Unlike other metal/zeolite combinations they retain high SCR activity and selectivity, even in the presence of excess water vapor. Another remarkable property of overexchanged Fe/MFI is its propensity to display the phenomenon of *catalytic oscillation* when catalyzing the decomposition of N_2O. As we showed in a previous paper (8), a gas mixture of N_2O (0.1%) in He that contains a critical concentration of H_2O vapor shows isothermal oscillations of the N_2O concentration in the effluent in the temperature range of 400–550°C. The frequency of this oscillation was found to be independent of the presence of O_2 or NO.

It is well known that Fe^{3+} ions in zeolite cavities can easily be reduced to Fe^{2+} and that this process is reversed by

[1] Schuit Institute of catalysis, Eindhoven University of Technology, P.O. Box 513, 3600 MB, The Netherlands.

[2] To whom correspondence should be addressed. Fax: 1-847-467-1018. E-mail: wmhs@nwu.edu.

0021-9517/00 $35.00

exposing the material to O_2 at elevated temperature (5, 9). Temperature-programmed reduction (TPR) with H_2 or CO shows that the reversible valence changes at temperatures below 500°C remain limited to the Fe^{2+}/Fe^{3+} couple (9); that is, the integrated TPR profile corresponds to the consumption of one H_2 or CO molecule per two Fe ions. Deeper reduction to Fe^0 requires higher temperatures and can be disregarded under the conditions of the present work. Oxidation of Fe^{3+} to Fe^{4+}, as claimed for the enzyme with binuclear Fe that can oxidize methane, has been discussed by Panov *et al.* for Fe/MFI, but was never proven for Fe/MFI with O_2 as the sole oxidant (10).

One issue that will be addressed in the present work is the oxidation of Fe/MFI by exposing it to N_2O. Panov *et al.* (10) reported that a special type of oxygen is formed in this way, which they call α-oxygen. This species was assumed to be responsible for the oxidation of benzene to phenol at room temperature. Although Fe^{4+} has been proposed for the enzymes of the methane methoxygenase group that oxidize methane to methanol, Siegbahn and Crabtree (11) show by DFT calculations that a peroxy bridge between two Fe^{3+} ions, Fe–O–O–Fe, is energetically more favorable. A second issue of this paper is the very existence of a binuclear iron complex in Fe/MFI at high metal loading. If such a complex is indeed instrumental for the N_2O decomposition catalysis, one should expect that the rate of this reaction increases in a nonlinear fashion when the Fe loading reaches a value where the binuclear complex is feasible. Kinetic data will therefore be shown of N_2O decomposition and the rate constant will be plotted against Fe loading.

EXPERIMENTAL

Sample Preparation

Samples were made from the protonic form of the parent zeolite with a nominal framework Si/Al ratio of 14 and 20, respectively, obtained from Degussa.

Fe/MFI samples have been prepared by two different methods: (i) sublimation of $FeCl_3$ into dehydrated zeolite as described previously (5) and (ii) solid-state ion-exchanged samples were produced by the procedure in which 2 g of H-MFI was first calcined under O_2 at 550°C for 4 h, then purged with Ar at the same temperature for 4 h, and transferred to a glove box without contact with air. After mixing in an agate mortar with the appropriate amount of $FeCl_2$ (Aldrich Chemical, 99.99% purity) under a dry N_2 (UHP) atmosphere, the mixture was transferred to the reactor and sealed. After placing this reactor into a furnace, it was exposed to a flow of Ar while being heated at a rate of 0.25°C/min to 550°C and held for 24 h at 550°C. Finally, the samples were washed to remove chlorine. For this purpose 2 g of the catalyst was stirred in 2000 ml of demineralized water for 10 h, and then the sample was filtrated and washed with water until the precipitation of AgCl was not detected upon the addition of $AgNO_3$ to the residual water. After drying in air, the samples were calcined for 4 h in flowing oxygen at 550°C.

TABLE 1

Basic Information on the Samples Studied

Sample designation (see text)	Preparation method	Si/Al	Fe/Al	Fe/uc[a]
Fe/MFI(1.37)			0.30	1.37
Fe/MFI(1.82)			0.40	1.82
Fe/MFI(2.50)	Solid state	20	0.55	2.50
Fe/MFI(4.20)			0.92	4.20
Fe/MFI(5.02)			1.10	5.02
Fe/MFI(6.40)	Sublimation	14	1.00	6.40

[a] Atomic ratio of Fe/uc. The unit cell (uc) contains 96 Td atoms (Si/Al).

Characterization. The iron content of the samples has been determined by the ICP method. Elemental analyses are shown in Table 1. The samples are designated as Fe/MFI(X), where X is the number of Fe atoms per unit cell of 96 tetrahedra. A small content of Cl is detected in the fresh samples and vanishes after brief use in a catalytic test run. The total Al/Si ratio is determined by chemical analysis; the number of Al ions in tetrahedral sites, $Al_{lattice}$, is equal to the number of protons in the parent H/MFI, detected by the IR band at 3610 cm^{-1}. The Fe/Al ratio, calculated from the decrease of the intensity of the 3620-cm^{-1} band upon adding Fe ions, is assumed to be equal to the $Fe/Al_{lattice}$ ratio.

X-ray powder diffraction patterns were recorded on a Siemens D500 diffractometer using Cu $K\alpha$ radiation. For temperature-programmed reduction (TPR), typically 200 mg of the sample was calcined at 500°C in flowing dry O_2 for 2 h, cooled to room temperature, and purged with He for $\frac{1}{2}$ h.The TPR experiments were then carried out in 2% CO /Ar at a total flow rate of 30 ml/min at 8°C/min. For quantitative evaluation of the TPR profiles, the amount of the consumed reductant was calibrated with CuO.

For FTIR analysis, samples were pressed into self-supporting wafers and measurements were performed between 4000 and 400 cm^{-1} on a Nicolet 60SX FTIR spectrometer equipped with a MCT detector. The wafers (10 mg) were mounted on quartz holders and introduced into a quartz cell. In a typical experiment the samples were pretreated up to 450°C under a flow of dry Ar for 2 h and then the IR spectra were recorded at 200 and 30°C. To achieve quantification, the intensity of this band was normalized for varying wafer thickness using the intensity of the zeolite overtone bands between 1800 and 1950 cm^{-1}.

ESR spectra were recorded on a Varian E-4 spectrometer at 9.3 Ghz (X band). The spectra were recorded at room temperature and at −196°C. The ESR signals were

registered at microwave power of 10 mW and modulation amplitude of 10 G in the field range of 50–6000 G. Typically, 40 mg of the oxidized samples was studied in their hydrated form.

Catalytic Tests

The N_2O decomposition was carried out in the temperature range of 350–550°C, using a standard flow reactor, GHSV = 42,000 h^{-1}, a mixture of N_2O (0.1–0.5%), O_2 (2–20%), and H_2O (3–15%) diluted with He (weight of catalyst, 200 mg; total flow, 280 $cm^3\,min^{-1}$). Typically, Fe/MFI samples were pretreated *in situ* in flowing 10% O_2 in He at 500°C (100°C/h) for 2 h before reaction. Gas chromatography was used to detect N_2, N_2O, and O_2. The catalytic activity was estimated by the conversion of N_2O to N_2. The reactor effluent was also analyzed by on-line quadrupole mass spectrometry (MS) using $m/e = 44$ for N_2O, $m/e = 28$ for N_2, $m/e = 32$ for O_2, $m/e = 46$ for NO_2, and $m/e = 30$ for NO. The MS had been calibrated for the pure gases, fully considering all fragmentation peaks.

A continuous-flow single-pass reactor was used for the kinetic studies. The rates r of N_2O decomposition were expressed as the number of micromoles of N_2 formed per second per gram of the catalyst; they were calculated from

$$r = C/(W/F(N_2O)).$$

Differential reaction rates were determined from linear plots of the fractional conversion, C, versus the space velocity, $W/F(N_2O)$, where W was the catalyst weight and $F(N_2O)$ the flow rate. Conditions were chosen so as to keep the conversion below 15%. The product ratio of N_2 to O_2 was always close to 2.0, corresponding to the reaction $N_2O = N_2 + \frac{1}{2}\,O_2$.

RESULTS

Fe/MFI after Preparation

Chemical analysis. The analysis of the calcined samples is reported in Table 1. The samples are designated as Fe/MFI(X), where X is the number of Fe atoms per unit cell of 96 tetrahedra.

X-ray diffraction (XRD). The XRD powder patterns of Fe/MFI samples show the presence of only a pentasyl-type framework structure characteristic of MFI (MFI zeolite); no evidence was found of damage to the zeolite structure or of the presence of an additional phase.

FTIR spectra. The interaction of the iron species with the zeolite has been probed using FTIR spectroscopy by exploring both the hydroxyl stretching (4000–3300 cm^{-1}) and framework vibration (1350–400 cm^{-1}) regions. The FTIR spectrum in Fig. 1a of H-MFI with Si/Al = 20 shows two bands in the OH stretching region after dehydration under

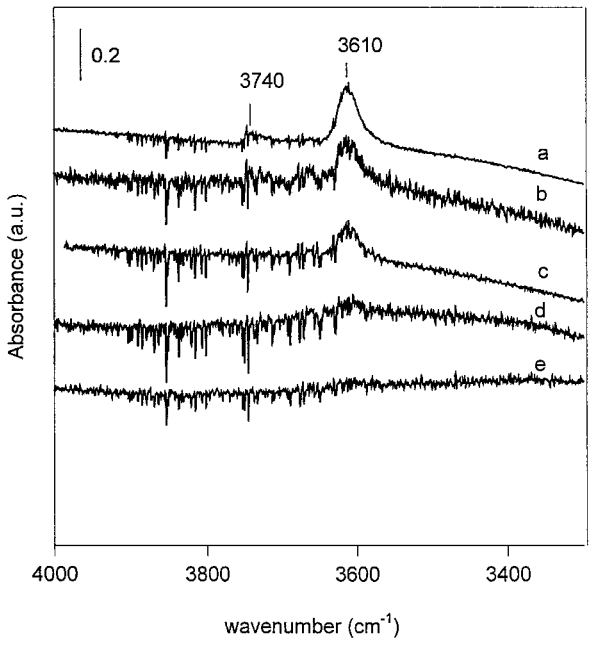

FIG. 1. FTIR spectra taken at 200°C of the hydroxyl stretching region: (a) H-MFI, (b) Fe/MFI(1.37), (c) Fe/MFI(2.50), (d) Fe/MFI(4.20), and (e) Fe/MFI(5.02).

a flow of dry Ar at 450°C for 2 h. The band at 3610 cm^{-1} is assigned to Brønsted acid groups associated with framework aluminum ((Si(OH)Al) (12, 13), while that at 3740 cm^{-1} is assigned to mononuclear silanol groups present in the channels and at the external surface. Upon introducing iron into cavities by solid-state ion exchange, the intensity of the bands at 3610 cm^{-1} decreased with increasing Fe loading (Fig.1, parts b–e). This is direct evidence for the exchange of protons by iron. In the case of Fe/MFI prepared by sublimation, about 30% of Brønsted acid sites is regenerated after subsequent hydrolysis and calcination. The presence of Fe in cationic sites induces a local deformation of the T–O–T bonds in the adjacent framework, as evidenced by the IR bands that are due to lattice vibration. These bands are in the region between 1200 and 400 cm^{-1}; in Fig. 2 the bands at 1230–1020 and 820–810 cm^{-1} are shown. Additional bands at 920 and 907 cm^{-1} are also observed. At low Fe loading (Fe/uc $\leq$ 2.50), the band caused by Fe perturbation at 920 cm^{-1} is observed (Fig. 2, parts b and c), while at higher Fe loading this band is shifted to 907 cm^{-1} (Fig. 2, parts d and e). Also in the overexchanged Fe/MFI(6.4) sample that was prepared by sublimation, an Fe-perturbed band is observed at 907 cm^{-1} (not shown). Bands near 1230–1220 cm^{-1} are assigned to internal asymmetric modes (14). Bands near 800 cm^{-1} have been attributed to both internal and external symmetric vibrations (14).

ESR spectra. The ferric ions observed in various zeolitic systems, including the present one, are usually in high spin $3d^5$ configuration (S = 5/2, ^6S being the ground state of the free ion).

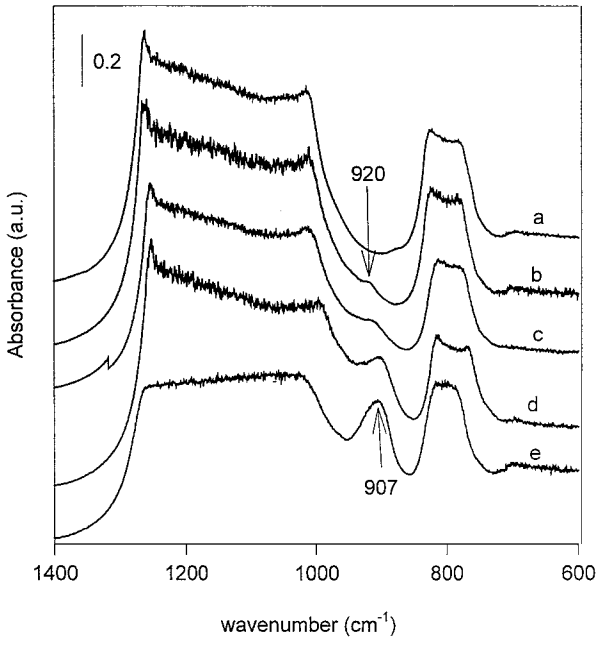

FIG. 2. FTIR spectra taken at 30°C of the Fe/MFI samples in the region 1400–600 cm^{-1}: (a) H-MFI, (b) Fe/MFI(1.37), (c) Fe/MFI(2.50), (d) Fe/MFI(4.20), and (e) Fe/MFI(5.02).

The *X*-band ESR spectra at −196 and +22°C of calcined Fe/MFI catalysts in their hydrated form are shown in Figs. 3 and 4, respectively. They are interpreted in terms of overlapping lines. At the lowest Fe^{3+} concentrations (Fe/uc < 2.50) a single, intense low-field line with a g value of 4.3 is observed (Fig. 3, Fig. 4, parts a and b). While the Fe^{3+} concentration increases (Fe/uc > 2.50), $g = 4.3$ persists, but new lines appear at $g = 6.3$ and $g = 5.6$. These new components are sensitive to dehydration and adsorption of probe molecules. Indeed, the dehydration of the sample increases their ESR intensity and the adsorption of ammonia leads to the disappearance of these two lines (not shown), indicating that the sites are distorted. The spectra taken at room temperature show characteristic differences (Fig. 4). In addition to the line observed at $g > 3$, other lines are visible at $g < 3$. In particular, all Fe/MFI samples prepared by solid-state ion exchange display broad lines at $g = 2.1$ with a peak-to-peak width (Δpp) of 1000 G, while the sample prepared by sublimation shows two broad lines at $g = 2.1$ with $\Delta pp = 1000$ G and a line at $g = 2.03$ with $\Delta pp = 450$ G. The intensity of these two lines at $g = 2.1$ and $g = 2.03$ does not follow Curie's law, which indicates that the ferric ions responsible for them are in mutual magnetic interaction. They should thus be part of small extraframework Fe–O clusters or tiny ferric oxide particles inside the zeolite channels, exhibiting super-paramagnetic or even ferromagnetic behavior. We attributed the lines observed in the low-field region ($g > 3$) to the presence of different mononuclear Fe^{3+} ions in a strong rhombic distortion of the tetrahedral site ($g = 4.3$) and to a less distorted

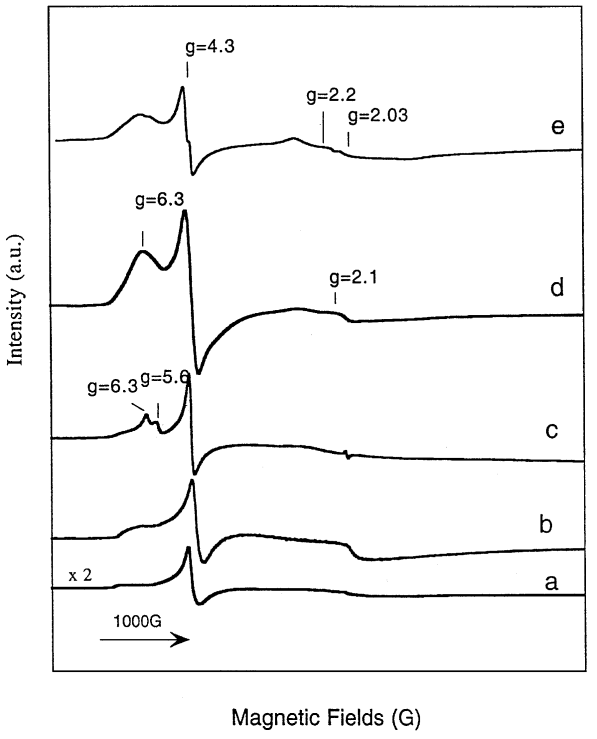

FIG. 3. ESR spectra of Fe/MFI samples recorded at −196°C: (a) Fe/MFI(1.37), (b) Fe/MFI(2.50), (c) Fe/MFI(4.20), and (d) Fe/MFI(5.02) and (e) Fe/MFI(6.40).

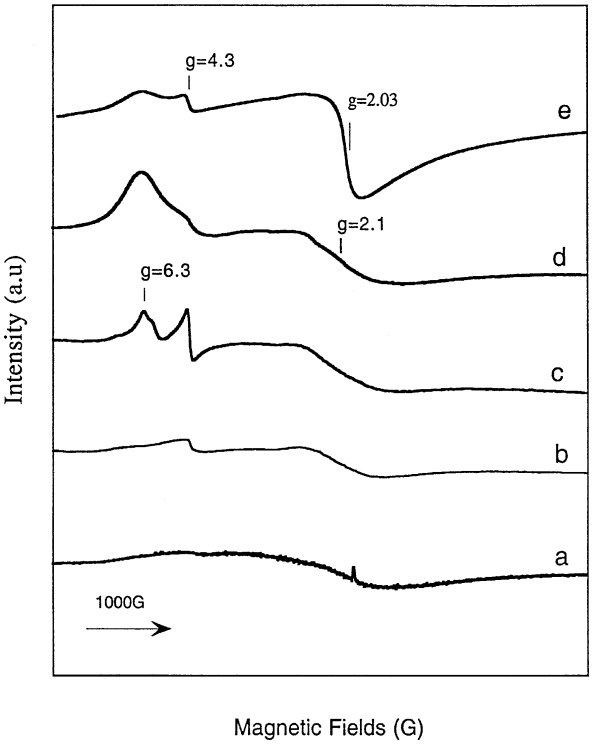

FIG. 4. ESR spectra of Fe/MFI samples recorded at 22°C: (a) Fe/MFI(1.37), (b) Fe/MFI(2.50), (c) Fe/MFI(4.20), and (d) Fe/MFI(5.02) and (e) Fe/MFI(6.40).

tetrahedron that maintains a C_{3v} axial symmetry ($g = 5.6$ and $g = 6.5$) (15). A detailed discussion of the line shapes of these signals can be found in the literature (16, 17). The lines at higher fields ($g < 3$), including the broad lines at $g = 2.1$ with $\Delta pp = 1000$ G, are attributed to the presence of clusters of α-Fe_2O_3 that were formed after washing and calcination of the catalyst. The band at $g = 2.03$ with $\Delta pp = 450$ G, which is only observed at room temperature but vanishes at $-196°C$, can be attributed to a separate antiferromagnetic Fe–O–Fe phase (9), such as the binuclear iron complex $(HO–Fe–O–Fe–OH)^{2+}$, or even to larger Fe–O–Fe clusters.

ESR spectra of Fe/MFI samples with different Fe loadings, after their use as a catalyst for N_2O decomposition, were registered both at room temperature and at $-196°C$. During the catalytic runs, these samples had been exposed to a flow of 10% H_2O, 4% O_2, 0.1% N_2O, and balance He at a GHSV = 42,000 h^{-1}. In comparison to the fresh samples, these ESR spectra reveal some changes. As Fig. 5 illustrates, these changes are most marked for the overexchanged Fe/MFI(6.4). The spectra can be analyzed by assuming the presence of two components. One has a signal at $g = 4.3$, which is more intense in the high Si/Al sample. This signal is attributed to a mononuclear Fe species. The second signal is the line at $g = 2.03$ and $\Delta pp = 650$ G, which is due to clustered ferric ions; it is depressed at $-196°C$. The effect of the recording temperature is clearly visible and indicates non-Curie law behavior of these extraframework clusters. The broad line at $g = 2.03$ with peak-to-peak width $\Delta pp =$ 650 G, observed with Fe/MFI of Si/Al = 14, and the line at $g = 2.1$ and $\Delta pp = 1000$ G, observed with Fe/MFI of Si/Al = 20, indicate that different clusters are formed. It appears that more mononuclear species are present in the high Si/Al sample than in the sample with a low Si/Al ratio. Although the results cannot be quantified yet, the lower intensity of the line at $g = 4.3$ (mononuclear species) indicates that, in Fe/MFI(6.40) after N_2O decomposition in the presence of H_2O vapor, the majority of the iron (about 85%) consists of distinct nanoclusters with a core such as –Fe–O–Fe–.

Adsorption Complexes on Fe/MFI

FTIR spectra. In Fig. 6 are shown the FTIR spectra obtained by exposing the oxidized or reduced Fe/MFI(6.40) sample with Si/Al = 14 to a dry flow of 10% N_2O in He at 200°C for 2 h. A pair of bands with maxima at 1620 and 1575 cm^{-1} is observed. These bands are not formed at lower partial pressure (<1%) of N_2O. Remarkably, these bands are absent in samples with a higher Si/Al ratio (Si/Al = 20) and different Fe loadings (Fe/uc = 1.37, 1.82, 2.50, 4.20, or 5.02) after exposure to the same gas flow at the same temperature for 4 h (not shown). However, the same bands are easily observed over all Fe/MFI samples upon simple exposure to a flow of 0.5% NO + 3% O_2 in He at 200°C for $\frac{1}{2}$ h (Fig. 6, parts b–f). The 1620-cm^{-1} band is slightly shifted to 1630 cm^{-1}(Fig. 6c) for the sample Fe/MFI(1.37). These bands have been assigned in the literature to surface nitro and nitrate groups (18, 19). These adsorbates are sometimes lumped together under the name "NO_y groups".

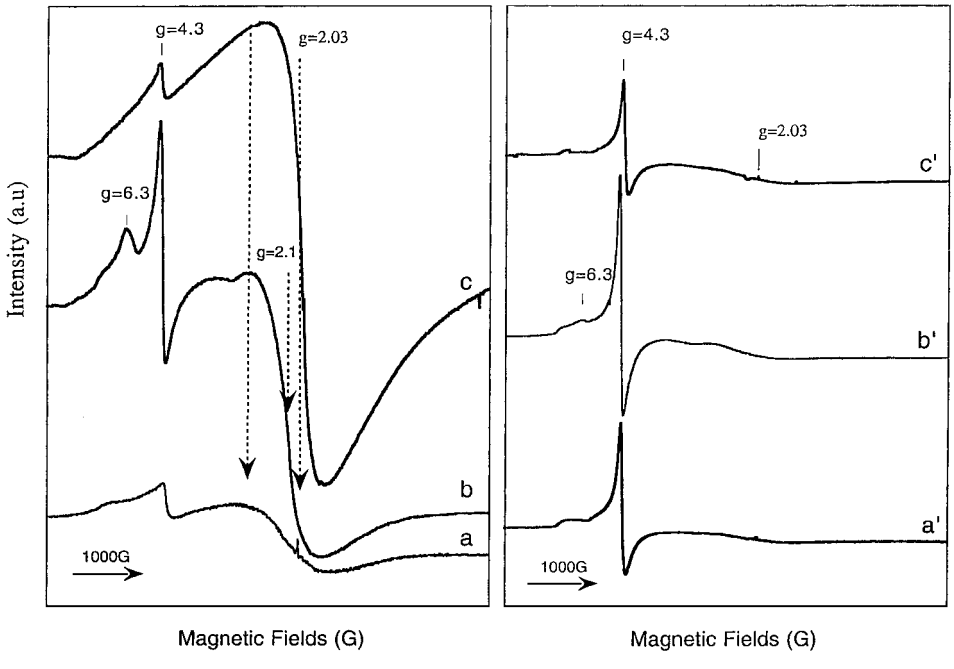

FIG. 5. ESR spectra of Fe/MFI samples used in N_2O decomposition in the presence of water vapor recorded at 22°C (a, b, c) and at $-196°C$ (a′, b′, c′): (a, a′) Fe/MFI(2.50), (b, b′) Fe/MFI(5.02), and (c, c′) Fe/MFI(6.40).

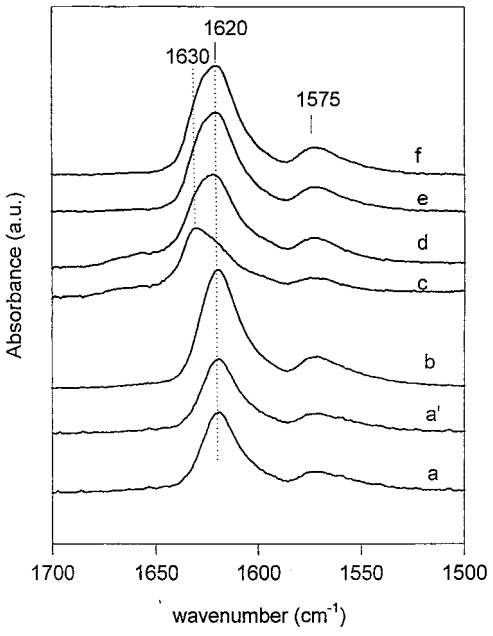

FIG. 6. FTIR spectra taken at 200°C of the nitro and nitrate species adsorbed on Fe/MFI: after exposing oxidized (a) and reduced (a′) Fe/MFI(6.40) to a flow of 10% N_2O in He at 200°C for 2 h, and after exposing oxidized Fe/MFI(6.40) (b), Fe/MFI(1.37) (c), Fe/MFI(2.50) (d), Fe/MFI(4.20) (e), and Fe/MFI(5.02) (f) to 0.5% NO in He + 3% O_2 in He at 200°C for $\frac{1}{2}$h.

More specifically, we assign the band at 1620–1630 cm^{-1} to a nitro group (20, 21) and the band at 1575 cm^{-1} to a nitrate ion (18–22, 23). It is well known that NO_y groups are formed when NO_2 interacts with transition metal ions in zeolite cavities, but their formation from N_2O is a new result of potential relevance to the chemistry of this catalyst system. As might be expected, a treatment with CO at 200°C for $\frac{1}{2}$ h of samples containing such NO_y groups leads to the disappearance of these bands (not shown), indicating that NO_y groups are highly reactive toward CO. These bands disappear also upon contacting the sample with benzene vapor at 200°C, indicating again their high reactivity. However, these bands remain intact when the sample is exposed to benzene vapor at room temperature.

CO-TPR. The adsorbed species formed on reduced Fe/MFI(6.40) upon exposure to a flow of 0.5% N_2O in He have been further identified by temperature-programmed reduction with CO. Figure 7 shows the CO_2 profiles. Also included in this figure is the CO-TPR profile of a sample that was merely exposed to O_2 at 500°C (Fig. 7a). This profile is clearly different from those of the samples that were exposed to 0.5% N_2O in He at a variety of temperatures (Fig.7, parts b–d). Whereas the profile of the sample exposed to O_2 peaks at 400°C, all Fe/MFI catalysts exposed to N_2O show one peak located near 300°C, irrespective of the temperature of this exposure. The integral of the CO_2 profile does, however, clearly increase with exposure temperature, indicating that the interaction of the reduced sample with N_2O is an activated process. The ratio CO_2/Fe, calculated from this integration, is ∼0.48 for the sample exposed to O_2 only, indicating reduction of Fe^{3+} to Fe^{2+}. In contrast, for the samples that had been exposed to N_2O at high temperature, the CO_2/Fe ratio is significantly higher, reaching a value of 0.65 for the sample exposed to N_2O at 320°C. The presence of additional oxygen, reactive toward CO, in the latter sample is consistent with the presence of peroxy groups Fe–O–O–Fe as predicted in Ref. 11.

TPD. In Fig. 8, temperature-programmed desorption (TPD) profiles are shown of the Fe/MFI(6.40) sample that had been first reduced and then exposed to flowing 0.5% N_2O in He at 320°C for 30 min, followed by purging with He for 2 h at room temperature. The desorbed gases were analyzed by mass spectrometry. A small amount of adsorbed N_2O is desorbed near 120°C in accordance with previous data, indicating that this process takes place well below 200°C (8). However, the major TPD products are NO and O_2, which are released at the same temperature near 340°C, indicating that they are decomposition products of the same ad-complex. Note that this sample had never been exposed to NO, so this formation of NO in the TPD profile is unambiguous proof that N_2O has been converted to a chemisorbed form of NO_x with $x = 2$ or 3. We saw from the FTIR data that the NO_y groups are stable up to 300°C; clearly, they decompose to NO and O_2. Figure 8 also shows an additional release of O_2 at $T > 450$°C. In this thermal reduction, some 12% of the iron in Fe/MFI(6.40) is reduced from Fe^{3+} to Fe^{2+} at $T \leq 550$°C.

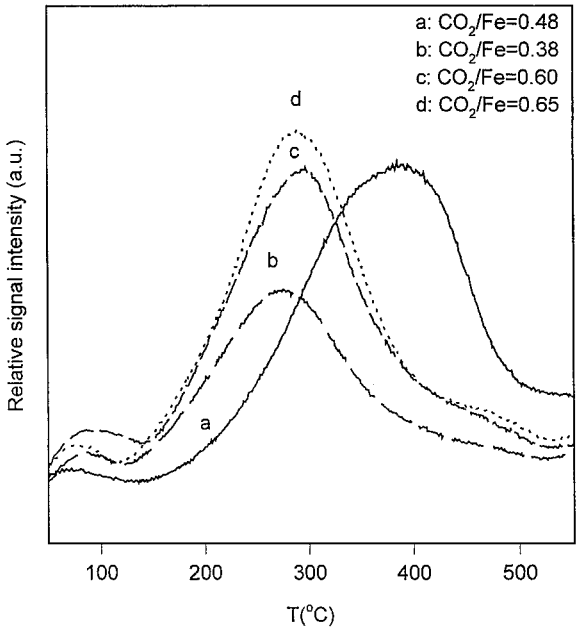

FIG. 7. CO-TPR after oxidation of reduced Fe/MFI(6.40) with either 100 kPa O_2 at 500°C for 2 h (a) or with 0.5 kPa N_2O at 200°C (b), 300°C (c), and 320°C (d) for $\frac{1}{2}$ h.

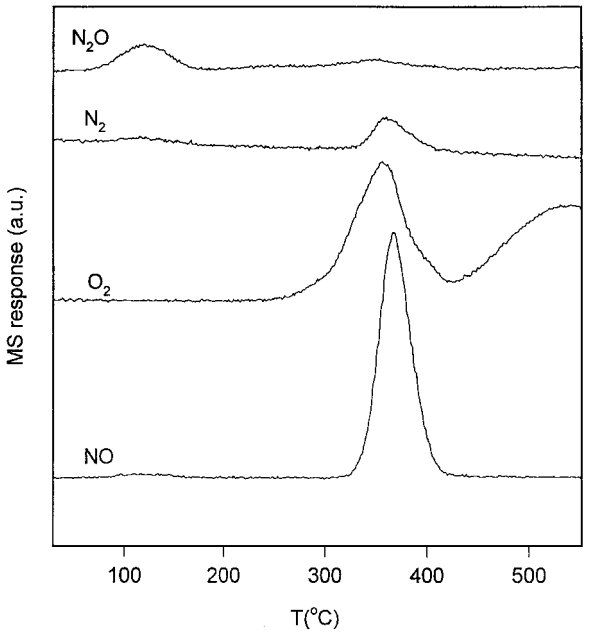

FIG. 8. TPD profiles after exposing reduced Fe/MFI(6.40) to 0.5% N_2O diluted in He at 320°C for $\frac{1}{2}$ h, followed by purging with He at 22°C for $\frac{1}{2}$ h.

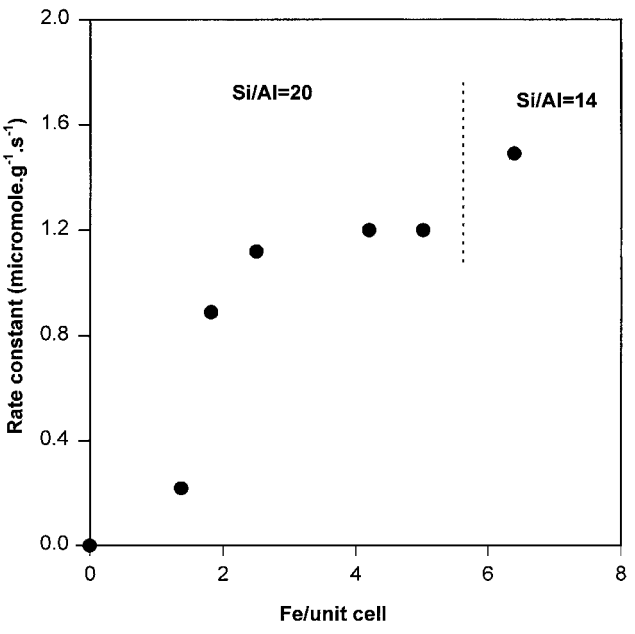

FIG. 10. N_2O decomposition over Fe/MFI: effect of Fe loading on the rate constant.

Kinetics of N_2O Decomposition

The effect of N_2O pressure on the rate of N_2O decomposition was studied at 400°C over the range of 0.15 to 0.4% N_2O in He. As a typical example, Fig. 9 shows the N_2 formation rate as a function of the partial pressure of N_2O in the feed for the Fe/MFI(4.20) catalyst. Clearly, a first-order dependence is found. In our previous paper we reported that addition of O_2 (2 to 10%) to the feed stream at different temperatures does not affect the rate of N_2O decomposition. No deactivation was found when the reaction was continued for more than 24 h in the absence or presence of added oxygen. These results established the rate expression as

$$\text{Rate}(N_2\text{ formation}) = kP(N_2O),$$

where k is the rate constant for 1 g of catalyst. In Fig. 10 this rate constant of N_2O decomposition at 400°C is plotted against the Fe loading of a number of Fe/MFI catalysts with Si/Al = 20 that were prepared by solid-state ion exchange. Clearly, the rate constant is very low for samples with low Fe content, but jumps to a much higher value above a critical Fe loading of Fe/uc = 1.82. Further increase of the Fe loading has only a small effect. An even higher value of the rate constant is found for the Fe/MFI(6.40) sample with higher Al content (Si/Al = 14). This nonlinear behavior of the rate constant is consistent with the model of a binuclear (or multinuclear) center. Once the probability is high for each Fe ion to find another Fe ion in its vicinity so that a binuclear oxygen-bridged complex can be formed, the rate of N_2O decomposition reaches a high value. Further increase of the Fe concentration has little effect on the decomposition rate. Recently, direct proof for the predominance of binuclear sites in Fe/MFI prepared by sublimation was obtained by EXAFS by the research groups of Prins and co-workers (24) and Koningsberger and co-workers (25). It stands to reason that this conclusion will also apply to catalysts containing high Fe loadings, prepared by solid-state ion exchange.

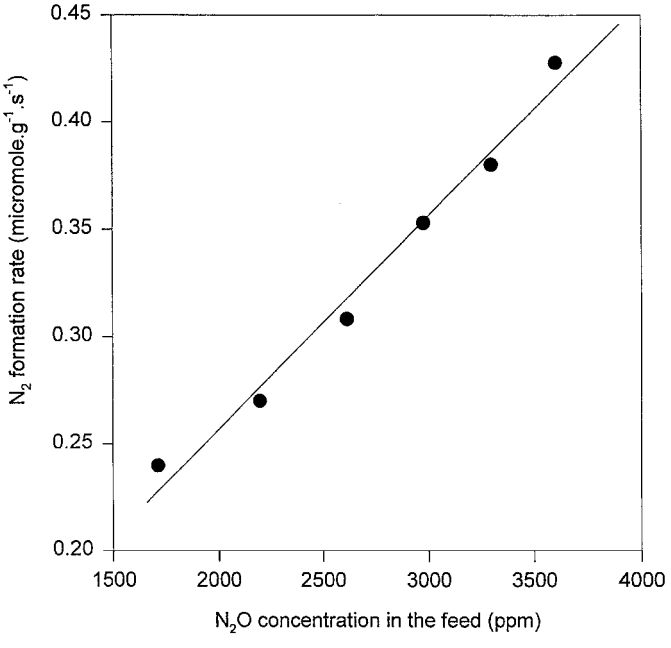

FIG. 9. N_2O decomposition over Fe/MFI(4.20): rate of N_2 formation at different N_2O inlet concentrations; T = 400°C.

TABLE 2

Performance of Fe/MFI Samples for Nitrous Oxide Decomposition at 500°C in Dry (Steps 1 and 3) and Wet (Step 2) Conditions

Samples	Si/Al	N_2O decomposition (%)[a]		
		Step 1[b]	Step 2[c]	Step 3[d]
Fe/MFI(2.50)	20	81	25	72
Fe/MFI(5.02)	20	100	32	72
Fe/MFI(6.40)	14	100	50–60[e]	90

[a] Average conversion of N_2O to N_2 taken after 24 h.
[b] Step 1: 0.1% N_2O in He, 4% O_2 in He, GHSV = 42,000 h^{-1}.
[c] Step 2: 0.1% N_2O in He, 4% O_2 in He, 10% H_2O, GHSV = 42,000 h^{-1}.
[d] Step 3: after return to similar conditions described in step 1.
[e] Instability.

To investigate the effect of water vapor on the activity of Fe/MFI samples for nitrous oxide decomposition, selected samples were tested for N_2O decomposition, first in the presence of O_2 for 24 h at 500°C (step 1), then after the addition of 10% H_2O vapor (step 2), and again in a dry feed (step 3). As can be seen from Table 2, the addition of 10% H_2O to the feed lowers the N_2O conversion. The results of transient experiments at 500°C between dry and wet conditions are also included in Table 2. They reveal that the N_2O conversion is highest (81–100%) in a dry feed (step 1) but decreases upon addition of water to the feed (step 2). Interestingly, the N_2O conversion over Fe/MFI(2.50) and Fe/MFI(5.02) with Si/Al = 20 decreases, but stabilizes at 25 and 32%, respectively. Over Fe/MFI(6.40) no real steady state is reached in the presence of H_2O and the conversion oscillates between 50 and 60%. In all Fe/MFI samples, the conversion did not return to the original value upon returning to the dry feed (step 3), but remained about 10 to 26% below the initial level.

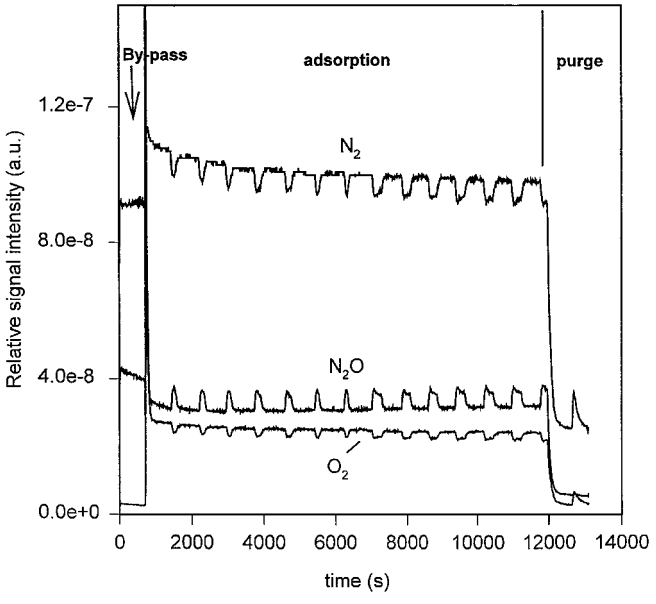

FIG. 11. Outlet concentrations vs time of N_2O, N_2, and O_2 in N_2O decomposition over Fe/MFI(6.40) at 500°C, GHSV = 42000 h^{-1}. Feed: 0.25% N_2O in He and 10% H_2O.

In view of the rather slow response of the GC analyzer, we decided to use mass spectrometry to follow the reaction rate under isothermal conditions in dry and wet atmospheres. We found that, in a dry feed, the concentrations of N_2O, N_2, and O_2 remain stable, but upon addition of 10% of H_2O vapor, the concentrations of reactants and products begin to oscillate. This is reproducible over Fe/MFI(6.40) with Si/Al = 14 (Fig. 11), but no oscillation is observed over Fe/MFI samples with a high Si/Al ratio (Si/Al = 20) or lower Fe loading (not shown).

For Fe/MFI(6.40), it takes 2–3 h after switching from the dry to the wet feed for regular oscillations to set in. The temperature of the catalyst bed remains constant during this run. At this temperature the average conversion remains constant at about 55% while the actual conversion oscillates between 60 and 50%. The peak-to-peak distance is about 800 s. During all oscillations, the N_2 and O_2 are formed in a strictly stoichiometric ratio. After purging with He at the end of reaction, only the desorption peaks of N_2 and O_2 ($N_2/O_2 = 2$) can be detected.

DISCUSSION

To maximize the extent of ion exchange, two methods were used in this work, namely, sublimation of $FeCl_3$ into the cavities of dry H-MFI and solid-state ion exchange of mixtures of $FeCl_2$ with dry H-MFI. In both cases the iron chloride reacts with the Brønsted acid sites, HCl is released, and $FeCl_2^+$ or $FeCl^+$ ions are attached to the zeolite lattice. In a subsequent hydrolysis step, the Cl ligands at the Fe are replaced by OH groups.

Nature and Localization of Fe Species

The FTIR data show that the interaction of H-MFI with $FeCl_3$ or $FeCl_2$ is stoichiometric: the Brønsted sites (band at 3610 cm^{-1}) are completely removed; i.e., ion exchange occurs and highly dispersed Fe complexes are formed. The presence of iron in cationic sites leads to perturbation of framework T–O–T vibrations because Fe ions are bonded to framework oxygens. The deformation of the T–O–T bonds gives rise to additional IR bands. At low Fe loading (Fe/Al < 0.55), the resulting band is located at 920 cm^{-1}, but at higher Fe loading (Fe/Al ~ 1) a band exists at 907 cm^{-1}. This difference indicates a different nature or location of the Fe^{3+} cations inside the zeolite cavities at low and high metal loading. The ESR data confirm this. At low Fe loading (Fe/Al < 0.55) only one kind of mononuclear Fe^{3+} species exists that gives rise to the $g = 4.3$ signal, indicating a strong rhombic distortion of the tetrahedral coordination of this Fe. But when the Fe loading increases, another mononuclear Fe^{3+} becomes visible with $g = 6.3$ and 5.6, suggesting

a less distorted tetrahedral coordination. Such species are found both after solid-state ion exchange and after sublimation. In the latter case, an additional broad band is observed at $g = 2.03$. In a previous paper, we argued that this is indicative for Fe^{3+} ions in strong magnetic interaction with each other (9). This suggests a binuclear complex or even a multinuclear Fe cluster. For the complex causing the line at $g = 4.3$ an $(HO{-}Fe{-}OH)^{+}$ ion in a cationic-exchange position appears to be a plausible structure, while the line at $g = 6.3$ and $g = 5.3$ can be attributed to $(Fe{=}O)^{+}$ because their intensity increases upon dehydration of the material. The temperature dependence of the $g = 2.03$ line in the sample prepared by sublimation is significant: this line disappears at the liquid nitrogen temperature. This antiferromagnetic characteristic shows that this species is a small cluster of Fe, such as a binuclear Fe complex. For metal loadings lower than those used in the present work, Wichterlová *et al.* (26) recently proposed that Co^{2+} and Cu^{2+} cations in MFI can occupy three kinds of positions: α at walls of the straight and sinusoidal channels and β and γ in five- and six-membered rings. These authors note that when Co or Cu ions are exchanged into MFI, the γ sites are filled first, then the β sites, and finally the α sites. Based on an IR study following the adsorption of NO over Fe/MFI zeolite, Lobree *et al.* (27) have indicated that Fe ions can occupy different positions inside the zeolite cavities. The present ESR results for Fe/MFI prepared by solid-state ion exchange show a similar dependence on the M/Al ratio: at low loading ($Fe/Al < 0.55$) only Fe^{3+} ions in cationic-exchange positions ($g = 4.3$) are visible, but at higher metal loading ($Fe/Al \approx 1$) the lines at $g = 6.3$ and $g = 5.3$ emerge. Using Wichterlová's terminology, we suggest that, at low loading with $Fe/Al < 0.55$, Fe fills primarily the γ and β sites. At higher loading the Fe^{3+} ions in distorted tetrahedral coordination ($g = 6.3$ and $g = 5.3$) are basically mononuclear species, possibly $(Fe{=}O)^{+}$. In addition, Fe clusters are formed, in particular in the sample prepared by sublimation followed by calcination. The ESR signal at $-196^{\circ}C$, and its disappearance at room temperature, indicate that bi- (or multi-) nuclear clusters with cores such as Fe–O–Fe are formed displaying typical antiferromagnetic interaction, i.e., a strong signal at room temperature that disappears at $-196^{\circ}C$. Additional information derived from the ESR data is the presence, in all samples, of broad lines at $g = 2.1$ ($\Delta pp = 1000$ G) of which the intensity decreases at $-196^{\circ}C$. This signal is attributed to the presence of some Fe_2O_3 particles.

Transformation of N_2O into Adsorbed Nitro and Nitrate Groups

The present finding that exposing reduced Fe/MFI of high Fe/Al ratio to N_2O leads to the formation of nitro and nitrate groups is of relevance to the chemistry of this system. It is remarkable that this chemical transformation was observed only with overexchanged Fe/MFI(6.40), but never with MFI of low Al content (such as $Si/Al = 20$) and consequently low Fe loading.

In previous work it was shown by Lei *et al.* (28), with overexchanged Cu/MFI, that copper is present in the oxidized state in binuclear oxoions such as $(Cu{-}O{-}Cu)^{2+}$ with an extralattice oxygen bridging over two Cu^{2+} ions. Over this catalyst NO is transformed to N_2O. Work in this laboratory showed that Cu^{+} is simultaneously oxidized to Cu^{2+}. The crucial step in this transformation is that two NO molecules that are adsorbed on the two Cu^{+} ions of the bimolecular complex react as follows,

$$[Cu{-}\square{-}Cu]^{2+} \overset{O=N \quad N=O}{\Rightarrow} N_2O + (Cu{-}O{-}Cu)^{2+}$$

where $\square$ stands for an oxygen vacancy. The feasibility of this reaction was confirmed by theoretical analysis of Goodman *et al.* (29). It follows from the principle of microscopic reversibility that such sites must also catalyze the reverse reaction in which nitrous oxide reacts with a bridging oxygen to nitric oxide. The present IR data (Fig. 6) and the TPD results indicate that this reaction takes place over oxidized Fe/MFI catalysts. The formation of the adsorbed NO_y complex (nitro and nitrate groups) from N_2O over Fe/MFI with high metal loading strongly suggests that also in this case a binuclear complex is crucial in mediating the interconversion between NO and N_2O:

$$N_2O + [HO{-}Fe{-}O{-}Fe{-}OH]^{2+} \Rightarrow [HO{-}Fe \; \overset{O=N \quad N=O}{\square} \; Fe{-}OH]^{2+}$$

After desorption, the NO molecules will react with another bridging oxygen atom and form NO_2. The bridging oxygen will be supplied, at sufficiently high temperature, by the decomposition of N_2O to $N_2{+}O_{ads}$. Adding up both reactions results in

$$2N_2O \rightarrow 2NO + N_2.$$

A homogeneous decomposition of N_2O at high temperature was reported as early as 1930 by Musgrave and Hinshelwood (30). The existence of a binuclear iron complex with bridging oxygen was previously suggested for Fe/Y zeolites by Boudart and co-workers (31, 32) from their FTIR and Mössbauer studies. The present ESR data show also that the crucial difference between the samples with $Si/Al = 20$ and 14 is that only in the latter sample with higher Al content the broad line at $g = 2.03$ with $\Delta pp = 450$ G is present, which is attributed to a distinct Fe–O–Fe phase such as a binuclear complex $(HO{-}Fe{-}O{-}Fe{-}OH)^{2+}$. The presence of such a complex requires more than one Al-centered tetrahedron for charge compensation. Based on a

Monte Carlo simulation procedure for the distribution of Al ions over the MFI structure, it has been reported that the maximum value for $(M{-}O{-}M)^{2+}$/Al is close to 0.30 for Si/Al = 12, while this value is 0.19 for Si/Al = 24. (33) We conclude that both the ESR evidence and the chemical evidence based on IR spectroscopy and mass spectrometric analysis of the TPD product indicate the existence of the binuclear complex. The implication that only such a binuclear complex can mediate the transformation between N_2O and $NO + NO_2$ is further confirmed by the present IR data, which show that no adsorbed nitro or nitrate groups are formed from N_2O over Fe/MFI samples that contain only mononuclear Fe^{3+} ions.

Mononuclear Fe^{3+} ions do, however, easily show the IR bands of the nitro- and nitrate groups, when exposed to a feed of NO and O_2 at 200°C. It follows that the binuclear complex is required as a mediator for the formation of such groups from N_2O. There is ample evidence that these adsorbed nitro and nitrate groups play an important role as intermediates for NO_x reduction by hydrocarbons over zeolite-supported transition metal catalysts (34–36).

The present results are also relevant to a different issue. It is known that the interaction of N_2O with Fe/MFI prepared by hydrothermal synthesis produces an extremely active surface oxygen species, so-called α-oxygen, that is capable of converting methane to methanol, ethane to ethylene, and benzene to phenol at room temperature. The precise nature of this α-oxygen is unknown, but the sites thought to activate N_2O are believed to be extraframework Fe complexes. The present work shows that highly reactive nitro and nitrate complexes are formed from N_2O. However, these complexes are not reduced by benzene at room temperature; therefore, they do not appear to be identical with "α-oxygen". Possibly a peroxo complex, Fe–O–O–Fe, such as that proposed by the calculations of Siegbahn and Crabtree (11), is a more plausible structure for α-oxygen.

N_2O Decomposition: Kinetics and Development of the Oscillation

N_2O decomposition to N_2 and O_2 has been studied for many years over various transition-metal-based catalysts. The rate of the reaction of N_2O decomposition over the present Fe/MFI catalysts is first order with respect to N_2O concentration; no inhibition by oxygen is observed in accordance with the literature data. The new finding is, however, that the rate constant increases in a nonlinear fashion with Fe loading, but changes little once the probability is high that each Fe ion finds one other Fe ion at a distance permitting formation with an oxygen-bridged binuclear complex. At very low Fe contents, mononuclear Fe species with low activity for this decomposition prevail. At high loading the rate constant is much higher, in particular with overexchanged Fe/MFI having a Si/Al ratio of 14.

We showed above that N_2O can not only oxidize the reduced binuclear sites by delivering bridging oxygen but also act as a reductant by consuming bridging oxygen and forming two NO ligands. Previously, this dualistic nature of the interaction between N_2O and zeolite-supported Fe was reported by Fu *et al.* (37). These authors studied the decomposition of N_2O over the fully oxidized form of Fe/Y and showed that N_2O has the ability of acting as either oxidant or reductant of the catalyst sites. A similar kinetic model has been proposed for the decomposition of N_2O over Cu/MFI involving binuclear Cu sites (28). Obviously, the delivery of an oxygen atom to a solid should be easier from N_2O than from O_2, which requires two adjacent sites that, in a zeolite, may be separated by a considerable distance. This may explain why O_2 does not suppress the rate of N_2O decomposition for such systems. For the overexchanged Fe/MFI where the presence of a binuclear complex is probable, the release of O_2 by interaction of N_2O with an oxidized site may be visualized as a two-step process: first, N_2O reacts with bridging oxygen to form a peroxide group, O_2^{2-}, without change in iron valency, as proposed by Siegbahn and Crabtree (11):

$$N_2O + \text{Fe–O–Fe} = N_2 + \text{Fe–O–O–Fe}.$$

In a subsequent step, the O–O unit is released as O_2, while the valency of each of the two iron ions is reduced by one unit. The assumption is based on results obtained with an enzyme that oxidizes methane. In this complex O_2 adds to $2Fe^{2+}$ to give O_2^{2-} and $2Fe^{3+}$. If this chemistry also holds for Fe/zeolites, then one of the two oxygen atoms in an Fe–O–O–Fe group could react with an organic molecule and the peroxide complex could be resurrected by an N_2O molecule, donating an O atom.

The formation of a complex with 2+ charge, as discussed above, requires two Al centered tetrahedra in each other's vicinity. This condition will be fulfilled for MFI with a low Si/Al ratio (Si/Al = 14), but not necessarily for samples where the overall Si/Al ratio is high. Indeed, the data in Fig. 10 show that the activity of Fe/MFI for N_2O decomposition varies with the Si/Al ratio in this sense. As shown above, the addition of water to the feed leads to a decrease of the activity (Table 2), which can be attributed to a competitive adsorption of H_2O and N_2O on the catalyst surface, both molecules being highly polar. Of greater interest is that the presence of water gives rise to regular, isothermal oscillations (Fig. 11). Such regular oscillations require some synchronization of processes by which each catalytic site oscillates between its two active forms. As there are no temperature oscillations found in this work, synchronization must be imposed by changes of the gas phase composition.

Previous investigators found oscillation of the N_2O concentrations during its decomposition over dry Cu/MFI. Giambelli *et al.* (38, 39) proposed a model for the

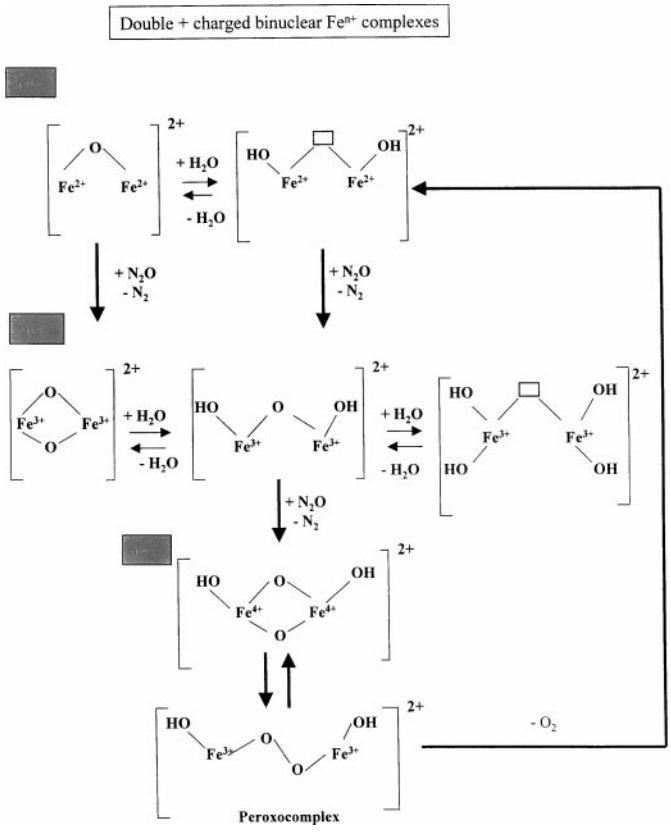

SCHEME 1

development of the oscillations based on the adsorption of nitrous oxide, the oxidation of monovalent copper, and the subsequent reduction of $(Cu{-}O{-}Cu)^{2+}$ pairs by N_2O. While this model is capable of predicting fluctuations in the nitrous oxide conversion, it does not take into account the role of nitric oxide, which was found to quench the oscillations. On the other hand, Turek and co-workers (40, 41) emphasized the importance of NO and also take the presence of adsorbed nitrate ions into account.

The present work shows that oscillations over Fe/MFI differ from those over Cu/MFI by the fundamentally different effect of water in the feed. Not only is water a prerequisite for oscillations to take place over Fe/MFI but also its concentration is critical. Increasing the moisture content of the feed to 15% leads to disappearance of the oscillation (not shown). Water vapor will control the number of OH ligands of any Fe ions and thus indirectly affect the reactivity of the sites. However, it is unclear at this stage how this coordination of the ions with OH ligands affects the oscillation frequency. The formation of well-defined multinuclear Fe clusters as evidenced by ESR seems to be responsible for the appearance of such an oscillation. Based on earlier EXAFS work, Joyner and Stockenhuber (42) proposed the formation of a multinuclear Fe cluster with the Fe_4O_4 structure in MFI; they state that such clusters cannot be reduced to the metallic state, even with hydrogen at 827°C, whereas interconversion between Fe^{2+} and Fe^{3+} is facile.

In Scheme 1 a possible rationalization for the observed development of oscillations in the presence of water vapor is illustrated during the catalytic decomposition of nitrous oxide over Fe/MFI. The mechanism shown is based on the analogy between the present binuclear Fe oxoions and similar ions detected in the enzymes that oxidize methane to methanol. In both cases, Fe^{2+} ions are oxidized by N_2O to Fe^{3+} and a second N_2O molecule deposits an additional oxygen atom on the binuclear Fe complex. For the resulting product, a twofold oxygen-bridged Fe^{3+} complex has been considered, but Siegbahn and Crabtree (11) have shown by density functional theory calculations that an isomeric peroxo complex is energetically more favorable. This complex can easily release an O_2 molecule, closing the catalytic cycle. Obviously, this cycle can function only if the H_2O pressure stabilizes the hydroxylated form of the O-bridged Fe^{2+} complex, as observed experimentally. This still leaves the question open as to which component of the gas phase might act as the synchronizing agent required for isothermal oscillations. No definitive answer can be given at this stage. Nitric oxide does not seem to have an effect on the development of oscillations. Its addition to the feed leads to an increased conversion of N_2O because NO removes oxygen from oxidized sites in a manner similar to that of CO.

CONCLUSIONS

1. Mononuclear Fe moieties, such as Fe^{n+} or $(FeO)^+$, are formed in MFI at low metal loading. At higher loading, in particular, in "overexchanged" samples prepared by sublimation or solid-state ion exchange, multinuclear Fe clusters (binuclear or larger) are present, displaying an antiferromagnetic signature at low temperature. In addition, a very broad ESR line indicates the presence of an unknown amount of iron oxide.

2. Binuclear sites and larger clusters are more active for N_2O decomposition than mononuclear sites. In addition, binuclear clusters catalyze the conversion of N_2O to NO and NO_2 and the reversed process. This chemistry results in the formation of nitro groups, NO_2^-, and nitrate groups, NO_3^-, conventionally lumped together as "NO_y groups" and identified by their IR bands.

3. Whereas such "NO_y groups" play an important role in NO_x reduction by hydrocarbons, their catalytic signature differs from that reported in the literature for the oxidation of methane to methanol and benzene to phenol with N_2O as the oxidant and hydrothermally prepared Fe/MFI as the catalyst.

4. Isothermal oscillations in the catalytic decomposition of N_2O to $N_2 + \frac{1}{2}O_2$ over Fe/MFI have been observed and are stable. Two conditions for such oscillations to occur are:

(1) a discrete pressure of H_2O and (2) high Fe loadings at which binuclear or larger clusters exist in the zeolite.

ACKNOWLEDGMENT

The authors gratefully acknowledge financial support by the NWO Spinoza Grant 1998 of the Royal Netherlands Academy of Sciences.

REFERENCES

1. Panov, G. I., Sheveleva, G. A., Kharitonov, A. S., Romannikov, V. N., and Vostrikova, L. A., *Appl. Catal.* **82**, 31 (1992).
2. Sobolev, V. I., Kharitonov, A. S., Paukshtis, Ye. A., and Panov, G. I., *J. Mol. Catal.* **84**, 117 (1993).
3. Feng, X., and Hall, W. K., *Catal. Lett.* **41**, 45 (1996).
4. Feng, X., and Hall, W. K., *J. Catal.* **166**, 368 (1997).
5. Chen, H.-Y., and Sachtler, W. M. H., *Catal. Today* **42**, 73 (1998).
6. Kapteijn, F., Marban, G., Rodriguez-Mirasol, J., and Moulijn, J. A., *J. Catal.* **167**, 256 (1997).
7. Sobolev, V. I., Panov, G. I., Kharitonov, A. S., Romannikov, V. N., Volodin, V. M., and Ione, K. G., *J. Catal.* **139**, 435 (1993).
8. El-Malki, El-M., van Santen, R. A., and Sachtler, W. M. H., *Microporous Mesoporous Mater.* **35–36**, 235 (2000).
9. El-Malki, El-M., van Santen, R. A., and Sachtler, W. M. H., *J. Phys. Chem. B* **103**, 4611 (1999).
10. Panov, G. I., Uriarte, A. K., Rodkin, M. A., and Sobolev, V. I., *Catal. Today* **41**, 365 (1998).
11. Siegbahn, P. E. M., and Crabtree, R. H., *J. Am. Chem. Soc.* **119**, 3103 (1997).
12. Woolery, G. L. Alemany, L. B., Dessau, R. M., and Chesler, A. W., *Zeolites* **6**, 14 (1986).
13. Dessau, R. M., Schmitt, K. D., Kerr, G. T., Woolery, G. L., and Alemany, L. B., *J. Catal.* **104**, 484 (1987).
14. Jasen, J. C., van der Gaag, F. J., and van Bekkum, H., *Zeolites* **4**, 369 (1984).
15. Bordiga, S., Buzzoni, R., Geobaldo, F., Lamberti, C., Giamello, E., Zecchina, A., Leofanti, G., Petrini, G., Tozzola, G., and Vlaic, G., *J. Catal.* **158**, 486 (1996).
16. Goldfarb, D., Bernanda, M., Strohmaier, K. G., Vaughan, D. E. W., and Thomann, H., *J. Am. Chem. Soc.* **116**, 6344 (1994).
17. Castner, T., Newell, G. W., Holton, W. C., and Slichter, C. P., *J. Chem. Phys.* **32**, 668 (1960).
18. Chen, H.-Y., Voskoboinikov, T. V., and Sachtler, W. M. H., *J. Catal.* **180**, 171 (1998).
19. Hadjiivanov, K., Knözinger, H., Tsyntsarski, B., and Dimitrov, L., *Catal. Lett.* **62**, 35 (1999).
20. Valyon, J., and Hall, W. K., *J. Phys. Chem.* **97**, 1204 (1993).
21. Adelman, B. J., Beutel, T., Lei, G.-D., and Sachtler, W. M. H., *J. Catal.* **158**, 327 (1996).
22. Busca, G., and Lorenzelli, V., *J. Catal.* **72**, 303 (1981).
23. Rochester, C. H., and Topham, S. A., *J. Chem. Soc. Faraday Trans. 1* **75**, 872 (1979).
24. Marturano, P., Drozdov, L., Kogelbauer, A., and Prins, R., *J. Catal.* **192**, 236 (2000).
25. Battiston, A. A., Bitter, J. H., Koningsberger, D. C., *Catal. Lett.* **66**, 75 (2000).
26. Wichterlová, B., Dědeček, J., and Sobalík, Z., *in* "Proceedings of the 12th International Zeolite Conference" (M. M. J. Treacy, B. K. Marcus, M. E. Bisher, and J. B. Higgins, Eds.), p. 941. Mater. Res. Soc., Baltimore, MD, 1998.
27. Lobree, J. L., Hwang, I.-C., Reimer, J. A., and Bell, T. A., *J. Catal.* **186**, 242 (1999).
28. Lei, G.-D., Adelman, D. J., Sárkány, J., and Sachtler, W. M. H., *Appl. Catal. B* **5**, 245 (1995).
29. Goodman, B. R., Schneider, W. F., Hass, K. C., and Adams, J. B., *Catal. Lett.* **56**, 183 (1998).
30. Musgrave, F. F., and Hinshelwood, C. N., *Proc. R. Soc. A* **135**, 23 (1932).
31. Garten, R. L., Delgass, W. N., and Boudart, M., *J. Catal.* **18**, 90 (1970).
32. Dalla Betta, R. A., Garten, R. L., and Boudart, M., *J. Catal.* **41**, 40 (1976).
33. Rice, M. J., Chakraborty, A. K., and Bell, A. T., *J. Catal.* **186**, 222 (1999).
34. Voskoboinikov, T. V., Chen, H.-Y., and Sachtler, W. M. H., *Appl. Catal. B* **19**, 275 (1998).
35. Voskoboinikov, T. V., Chen, H.-Y., and Sachtler, W. M. H., *J. Mol. Catal. A* **155**, 155 (2000).
36. Chen, H.-Y., Voskoboinikov, T. V., and Sachtler, W. M. H., *J. Catal.* **186**, 91–99 (1999).
37. Fu, C. M., Korchak, V. N., and Hall, W. K., *J. Catal.* **68**, 166 (1981).
38. Giambelli, P., Garufi, E., Pirone, R., Russo, G., and Santagata, F., *Appl. Catal. B* **8**, 331 (1996).
39. Giambelli, P., Di Benedetto, A., Garufi, E., Pirone, R., and Russo, G., *J. Catal.* **175**, 161 (1998).
40. Lintz, H.-G., and Turek, T., *Catal. Lett.* **30**, 313 (1995).
41. Turek, T., *J. Catal.* **174**, 98 (1998).
42. Joyner, R., and Stockenhuber, M., *J. Phys. Chem. B* **103**, 5963 (1999).